



Cyto/myeloarchitecture of cortical gray matter and superficial white matter in early neurodevelopment: multimodal MRI study in preterm neonates

Shiyu Yuan^{1,†}, Mengting Liu^{1,†}, Sharon Kim ^{1,†}, Jingda Yang¹, Anthony James Barkovich², Duan Xu², Hosung Kim ^{1,*}

¹Department of Neurology, USC Stevens Neuroimaging and Informatics Institute, Keck School of Medicine, University of Southern California, Los Angeles, CA 90033, USA,

²Department of Radiology & Biomedical Imaging, University of California, San Francisco, San Francisco, CA 94143, USA

*Corresponding author: 2025 Zonal Ave, Los Angeles, CA 90033, USA. Email: hosung.kim@loni.usc.edu

†These authors contributed equally to the study

The cerebral cortex undergoes rapid microstructural changes throughout the third trimester. Recently, there has been growing interest on imaging features that represent cyto/myeloarchitecture underlying intracortical myelination, cortical gray matter (GM), and its adjacent superficial white matter (sWM). Using 92 magnetic resonance imaging scans from 78 preterm neonates, the current study used combined T1-weighted/T2-weighted (T1w/T2w) intensity ratio and diffusion tensor imaging (DTI) measurements, including fractional anisotropy (FA) and mean diffusivity (MD), to characterize the developing cyto/myeloarchitectural architecture. DTI metrics showed a linear trajectory: FA decreased in GM but increased in sWM with time; and MD decreased in both GM and sWM. Conversely, T1w/T2w measurements showed a distinctive parabolic trajectory, revealing additional cyto/myeloarchitectural signature inferred. Furthermore, the spatiotemporal courses were regionally heterogeneous: central, ventral, and temporal regions of GM and sWM exhibited faster T1w/T2w changes; anterior sWM areas exhibited faster FA increases; and central and cingulate areas in GM and sWM exhibited faster MD decreases. These results may explain cyto/myeloarchitectural processes, including dendritic arborization, synaptogenesis, glial proliferation, and radial glial cell organization and apoptosis. Finally, T1w/T2w values were significantly associated with 1-year language and cognitive outcome scores, while MD significantly decreased with intraventricular hemorrhage.

Key words: cortical surface; cyto/myeloarchitecture; DTI; preterm neonates; T1w/T2w ratio.

Introduction

Human brain maturation involves complex morphological changes of the cerebral cortex, including the expansion of white matter (WM) and gray matter (GM), thickness, surface area, and folding. Alterations of such cortical morphological properties, which can be characterized by magnetic resonance imaging (MRI), have been associated with neuropsychiatric (Sierra et al. 2014; Li et al. 2016) and developmental disorders (Ecker et al. 2009; Pacheco et al. 2015) that originate in prenatal and postnatal periods. Such critical period of cortical development involves neuronal migration from the germinal matrix, rapid growth of pyramidal cells, synaptogenesis, and myelination, which establish cerebral connectivity and facilitate rapid synchronized communication among different brain regions (Laule et al. 2007).

Studies to date have demonstrated that brain myelination involves the transition from the premyelination to the myelination stage when immature oligodendrocytes proliferate and initiate myelogenesis through axon contact and wrapping (Back et al. 2001). These myelination events start during the late second or

early third trimester in the brainstem and deeper brain structures, eventually progressing to more peripheral brain regions to include superficial cerebral WM tracts. Alongside, these myeloarchitectural changes include precisely tuned cytoarchitectural events, including neural apoptosis, radial glial proliferation, dendritic arborization, neurite (neurons, axons, and dendrites) outgrowth and lamination, and synaptogenesis (Mrzljak et al. 1988; Rakic 2003). Recently, there has been increased spotlight on imaging features representing the underlying cortical cyto/myeloarchitecture that drives intracortical myelination and maturation of GM and its adjacent superficial white matter (sWM) (Grydeland et al. 2013; Phillips et al. 2013; Wu et al. 2014; Shafee et al. 2015; Oyefiade et al. 2018; Timmler and Simons 2019; Uddin et al. 2019; Kirilina et al. 2020; Norbom et al. 2020). Indeed, disruptions of cyto/myeloarchitectural events may lead to pathological outcome and are important prognostic indicators of response to perinatal injuries (Volpe 2009; Hinojosa-Rodriguez et al. 2017). Impaired myelination and immature WM are also associated with abnormal neurodevelopment, preterm birth, and perinatal insults

(Inder et al. 2005; Volpe et al. 2011; Ortinau and Neil 2015). The precise temporospatial pattern of cortical cyto/myeloarchitectural events in cortical GM and its adjacent sWM throughout the critical time frame of the third trimester, however, remain unclear.

Myeloarchitectural patterns can be characterized in vivo using multicontrast T1-weighted (T1w) and T2-weighted (T2w) MRI intensity values that may vary along with changes of water molecules and tissue macromolecules composing brain myelin (Clark et al. 1992; Barkovich 2005; Laule et al. 2007). Use of the semi-quantitative ratio of T1w/T2w signal intensity enhances the sensitivity and contrast to myelin, while reducing intersubject signal intensity bias (Glasser and Van Essen 2011) and has been helpful in studying brain connectivity (Ma and Zhang 2017) and cortical myelin maps (Van Essen et al. 2013; Glasser et al. 2014) in infants (Lee et al. 2015; Chen et al. 2017; Soun et al. 2017), healthy subjects (Grydeland et al. 2013; Shafee et al. 2015; Chopra et al. 2018), and aging adults (Teubner-Rhodes et al. 2016) and in clinical populations (Chao et al. 2015; Iwatani et al. 2015; Nakamura et al. 2017). Though, this imaging feature has yet to be employed in the analysis of preterm neonatal cortical development throughout the third trimester, as most developmental studies have only explored myeloarchitectural evolution from infancy to childhood and adulthood (Brody et al. 1987; Deoni et al. 2015).

The T1w/T2w intensity ratio, however, is not specific solely to myelination events and may reflect a combination of various cytoarchitectural changes associated with neurite (e.g. neurons and axons) proliferation and integrity. Thus, to enhance the specificity of information inferred, directional diffusivity measurements of diffusion tensor imaging (DTI) together with T1w/T2w signal intensities have the potential to distinguish among the variety of cyto/myeloarchitectural events. DTI generates metrics that are sensitive to the movement of water molecules, including fractional anisotropy (FA), mean diffusivity (MD), axial diffusivity (AD), and radial diffusivity (RD) (Supplementary Table S1) (Anjari et al. 2007; Counsell et al. 2008; Beaulieu 2014; Duerden et al. 2015).

While tract-based analyses of DTI have been investigated in preterm and term neonates, myelination and axonal development in cortical GM and sWM remain largely incompletely explored. A few studies have described serial quantitative measures with MRI in very preterm and healthy human infants (Counsell et al. 2002; Nossin-Manor et al. 2013; Schneider et al. 2016). However, these studies assessed myelination or axonal development visually (Counsell et al. 2008) or quantitatively but in only several WM and GM regions of interest (ROIs), which were sampled using manually placed landmarks (Anjari et al. 2007; Smyser et al. 2016). Furthermore, various DTI techniques have been used to understand cortical microstructural maturation and regionally specific signatures (Huppi et al. 1998; Ball et al. 2013; Pecheva et al. 2018; Batalle et al. 2019),

but the distinct differences in developmental trajectories between GM and sWM have not been thoroughly explored, especially in conjunction with other parameters sensitive to cyto/myeloarchitectural events, including T1w/T2w values. Likewise, a recent study explored cortical microstructural maturation in preterm neonates using FA and DTI mean kurtosis, but the measurements' precise relation to timing and specificity of cyto/myeloarchitectural events remain unclarified (Ouyang, Jeon, et al. 2019).

To attain a more complete picture of brain maturation, our study analyzed multimodal MRI features using combined features of T1w/T2w intensity ratio and DTI measurements. We aimed to characterize cortical cyto/myeloarchitecture of preterm neonates scanned in the equivalent age of the third trimester. First, we plotted the developmental trajectory of both cortical GM and sWM. Second, using a cortical ROI approach, we constructed differential spatiotemporal maps of T1w/T2w and DTI to characterize regionally specific signatures of GM and sWM across the cerebral cortex. Third, we examined the relationship between T1w/T2w and DTI measures to better define the differential microstructural properties. And finally, we examined whether T1w/T2w and DTI measures are associated with neurodevelopmental outcome and clinical conditions. We hypothesized that (i) the cyto/myeloarchitectural properties inferred by T1w/T2w and DTI would be different in sWM and GM and that (ii) T1w/T2w and DTI developmental trajectories are regionally distinct and indicative of spatiotemporally dependent developmental events of the cerebral cortex. With the goal of addressing the paucity of cyto/myeloarchitecture studies in the developing neonatal brain, our study importantly identifies microstructural changes that may provide a foundational understanding on neurodevelopment and clinical outcome.

Materials and methods

Participants

Our dataset includes 78 preterm neonates (mean post-menstrual age at birth [PMA]: 28.23 ± 2.07 weeks; range: 24–32 weeks) admitted to UCSF Benioff Children's Hospital San Francisco between June 2011 and March 2019. Neonatal demographic and clinical information are provided in Table 1. All patients were scanned postnatally as soon as they were clinically stable (PMA at scan: 33.10 ± 1.88 weeks; range: 28.80–35.70 weeks), and 39 patients were scanned again before discharge at late preterm age (PMA at scan: 37.31 ± 1.70 weeks; range: 33.14–41.98 weeks). However, many follow-up scans were excluded due to large motion artifact after quality control, resulting in a total of 92 T1w and T2w MRI scans and DWI scans (78 baseline, 14 follow-up scans). Other exclusion criteria included (i) clinical evidence of a congenital malformation or syndrome, (ii) congenital infection, and (iii) newborns clinically unstable for transport

Table 1. Demographic and clinical characteristics for preterm neonates.

Demographic	
Subjects (n)	78
Sex: males (n)	39
MRI scans (n)	92
GA at birth (weeks, mean \pm SD)	28.23 \pm 2.07
PMA at MRI	
First scans	33.10 \pm 1.88
Second scans	37.31 \pm 1.70
Characteristic ^a	
Maternal/antenatal factors	
Maternal age, years	31.56 \pm 7.46
Placenta previa	4 (7.27)
Drug abuse ^b	11 (17.74)
Magnesium sulfate	52 (77.61)
Exposure to prenatal steroids	63 (88.73)
Chorioamnionitis	11 (17.74)
Delivery/perinatal factors	
Twin	30 (40.54)
Birth weight (g)	1092.54 \pm 355.94
Cesarean section delivery	50 (67.57)
Postnatal factors	
Exposure to postnatal steroids	7 (10.45)
Hypotension	37 (53.62)
Infant infection ^c	45 (62.50)
PDA ^d	30 (48.39)
NEC ^e	5 (7.25)
Duration of intubation, days	9.12 \pm 14.99
CLD	17 (24.64)
Seizures	1 (1.45)
Pneumothorax	1 (1.45)

^aData presented as number (%), or mean \pm standard deviation. ^bAll subjects with maternal smoking (based on self-report) were exposed to marijuana, and 2 were also exposed to tobacco. ^cNewborns with culture-positive sepsis, clinical signs of sepsis with negative blood culture, or meningitis were classified as having infection. ^dNewborns with clinical signs of PDA (prolonged systolic murmur, bounding pulses, and hyperdynamic precordium) and evidence of left-to-right flow through the PDA on echocardiogram were classified as having a PDA. ^eIt was diagnosed based on Bell's stage II criteria (Kliegman et al. 1982); "Numbers and percentages were derived from 78 preterm subjects whose data was recorded and known."

to the MRI scanner. Parental consent was obtained for all cases following a protocol approved by the Institutional Committee on Human Research.

MRI and DTI acquisition

All participants underwent a brain MRI on a 3T GE Healthcare Discovery MR750 scanner. Infants were scanned under natural sleep after feeding. Sedation was used only with parental consent and when subjects initially moved to cause imaging artifact. Approximately, 25% of subjects received sedation usually pentobarbital in small doses. T1-weighted images were also acquired using sagittal 3D IR-SPGR (inversion time of 450 ms; FOV = 180 \times 180 mm²; NEX: 1.00; FA: 15°) and were reformatted in the axial and coronal planes, yielding images with 0.7 \times 0.7 \times 1 mm³ spatial resolution. Diffusion-weighted images were obtained using a single shot echo-planar sequence: 27 noncollinear diffusion gradients with a *b*-value of 1,000 s/mm², 3 nondiffusion-weighted (*b*₀) volumes, echo/repetition time: 80/8,000 ms, voxel size: 1.56 \times 1.56 \times 3 mm³, and acquisition time: 4:08 min. An anatomical T2-weighted sequence (3D Cube) was

also acquired: echo/repetition time: 65/2,500 ms, voxel size: 0.63 \times 1 \times 0.63 mm³, and acquisition time: 3 min, 20 s.

MRI-based diagnosis of neonatal brain injuries

A pediatric neuroradiologist (A.J.B.) who was blinded to patient history reviewed patient MRI scans, including 3D T1- and axial T2-weighted sequences, as well as susceptibility-weighted imaging when available. Presence and severity of 3 leading drivers of neurodevelopmental deficits, i.e. intraventricular hemorrhage (IVH), ventriculomegaly (VM), and periventricular leukomalacia (PVL) or white matter injury (WMI), were visually scored (Table 2). Subsequently, IVH scores were binarized with "mild," representing grades 1–2, and "severe," representing grades 3–4; PVL/WMI and VM were categorized as "mild" for grade 1 and as "severe" for grades 2–3. We merged infants with mild injuries and those with no injury into 1 none-mild injury group since the mild injury and no-injury groups exhibited no significant differences in the following analyses as well as in previous studies (Kim, Gano, et al. 2016; Kim et al. 2020).

Neurodevelopmental outcome assessment

All infants were referred to the UCSF Intensive Care Nursery Follow-Up Program upon discharge for routine neurodevelopmental follow-up. Neurodevelopment was assessed using the Bayley-III, which was performed by unblinded pediatric psychiatrist at 12, 18, and 30 months'-corrected age. Follow-up was available in 26 of the 78 infants (33%).

MR image processing of T1w and T2w imaging data

Three types of brain tissues (GM, WM, and CSF) were segmented using a joint label fusion method on T1w images. Next, the cortical surfaces of neonates were extracted from the segmentation using NEOCIVET pipeline (Kim, Lepage, et al. 2016; Liu et al. 2019). T2w images were then registered to the preprocessed T1w image using a rigid-body registration based on the similarity measure as mutual information. The registration results are exemplified in Supplementary Fig. S1 presenting individually paired T1w and DTI-FA maps at different ages. Then, T1w/T2w ratio was computed using the manner introduced in a previous study (Glasser and Van Essen 2011) and was sampled at vertices on the midcortical surface (=surface placed at the middle between GM/WM and GM/CSF borders) and the sWM surface (=surface placed at 2 mm below the GM/WM border), which were triangulated with 81,924 vertices (163,840 polygons). These features were further resampled to the surface template using the transformation obtained in the surface registration to allow intersubject spatial correspondence.

Table 2. Definition and categorization of clinical variables for statistical analysis. Clinical characteristics were fully available for 71 subjects among all the 78 subjects included in the study.

Factors	Definition	Grouping	
IVH	Bleeding into the ventricles of the brain (Chadha et al.)	Grades 0–2, none-mild (82)	Grades 3 and 4, severe (10)
VM	Dilatation of the lateral cerebral ventricles usually defined as >10 mm at the level of the atria (Mehlhorn et al. 2017)	Grades 0 and 1, none-mild (90)	Grades 2 and 3, severe (2)
PVL or WMI	Type of brain damage that affects the brain's WM and can lead to a series of disabilities, including cerebral palsy (Volpe 1997)	Grades 0 and 1, none-mild (83)	Grades 2 and 3, severe (9)
Birth weight	Gram	>=1,500 (8)	1–1,500 (63)
		>=1,000(46)	1–1,000 (25)
Birth age	Weeks	>=31 (3)	<31 (68)
		>=28(35)	< 28 (36)
Days intubated	Mechanical ventilation and intubation	0–5 (42)	>=5 (29)
PDA	An opening between the aorta and pulmonary artery	No (31)	Yes (40)
CLD	Long-term breathing and lung problems in premature babies	No (52)	Yes (19)
NEC	Inflammation of intestinal tissue that may cause perforation	No (67)	Yes (4)
Neonatal infection	Culture + or –sepsis and/or meningitis	No (26)	Yes (45)
Postnatal steroids	Exposure to postnatal hydrocortisol	No (63)	Yes (8)
Hypertension	Requiring treatment with volume resuscitation and/or vasopressors	No (36)	Yes (35)

DTI processing

Motion artifacts and eddy current distortions in DTI data were first corrected by normalizing each directional volume to the b_0 volume using FMRIB's Linear Image Registration Tool with 6 degree of freedom (Smith et al. 2004). The diffusion tensor was then calculated using a simple least square fit of the tensor model to the diffusion, and MD, AD, RD, and FA maps were then generated.

To accurately estimate the intracranial correspondence between structural- and diffusion-weighted image spaces, a label-fusion approach (Wang and Yushkevich 2013) was used to mask out noncortical structures for T1w and T2w images. The b_0 images were initially skull-stripped using Brain Extraction Tool (Smith 2002). Given that regional intensity and geometric differences exist between T2w and b_0 MR images (Klein et al. 2009), the ANTs software, a diffeomorphic mapping method with mutual information as the similarity measure, was used to warp the b_0 images to T2 images. Based on the estimated transformation parameters in the rigid registration between T2w and T1w images, b_0 volume (together with MD and FA volumes) was further transformed to T1 space for mapping the diffusion data on midcortical and sWm surfaces. Thus, FA, AD, RD, and MD values were sampled on the midcortical and sWm surfaces for further intersubject comparisons.

Regional analysis of T1w/T2w ratio and DTI parameters

In this study, we use the surface-based parcellation in which vertices that belong to the same anatomical structure are grouped. Here, we used the automatic anatomical labeling parcellation (Tzourio-Mazoyer et al. 2002) mapped to the neonatal cortical template using

the method described and evaluated in Kim, Lepage, et al. (2016) to define cerebral cortical GM and sWm ROIs. After the surface registration, 81,924 vertices that were sampled on each individual surface were labeled into 76 ROIs. We then calculated the average of each of T1w/T2w and DTI parameters sampled at vertices within each of 76 ROIs for each individual scan. These ROI mean features were used to analyze the pattern of spatiotemporal brain maturation from 28 to 42 gestational weeks (GW).

Spatiotemporally varying pattern of developmental trajectory

To evaluate the trajectory of cyto/myeloarchitectural maturation, linear mixed-effect regression models that addressed for repeated measurements (i.e. some subjects were scanned twice) were established for each T1w/T2w ratio, MD, AD, RD, or FA value as the dependent variable. In the models, we correlated each brain maturation metric with PMA at scan while including the following covariates as other independent variables: PMA at birth and sex. We analyzed these regression models for the whole cortex and 76 cortical regions. Due to the nonlinear trend observed in T1w/T2w values, we conducted a quadratic (=second polynomial) regression model across the cohort, which resulted in smaller fitting errors than the linear model for this measurement. Due to the nonlinear trend observed in T1w/T2w values, an Akaike information criterion (AIC) (Akaike 1981) was used to determine whether a linear regression or a quadratic (=second polynomial) regression model would best fit the data. Results indicated that quadratic fitting yielded lower AIC values for both midcortical and sWm surfaces. We thus conducted a quadratic regression model across the cohort for T1w/T2w values.

k-mean clustering to classify the cortical regions with respect to maturation rates and degrees

To facilitate the interpretation of the spatiotemporal maturation trajectory, we applied *k*-mean clustering to each imaging feature's temporally changing map that was estimated using the aforementioned mixed-effect regression models. Using this unsupervised learning method, we classified the 76 cortical ROIs into 2 groups according to their 2 regional developmental characteristics: individual feature value at the term equivalent age of 40 GW and the coefficient of feature value representing the maturation rate with respect to PMA across the cohort. Thus, the output of the *k*-mean clustering labeled all the 76 ROIs into either fast or slow maturation based on their maturation rate during the third trimester and the maturation level at term equivalent age. We determined the number of clusters using a cluster scheme quality index (SQI) (Halkidi et al. 2000), which selected the optimal *k* based on the ratio of intracluster distances (i.e. how close members of a cluster are to the class centroid) and intercluster distances (i.e. how far apart the clusters are). We chose the *k* that maximized the class discrimination factor $\lambda = 1/\text{SQI}$. As the solution might be influenced by the initialization, we repeated the clustering for 10,000 times to verify robustness. We chose the number of clusters *k* to be 3 because, at *k*=3, we achieved the highest-class discrimination factor λ . The second highest λ was achieved when using *k*=2, the results of which are also reported in [Supplementary Fig. S2](#).

Effects of perinatal clinical factors on developmental trajectory

We aimed to assess effects of each of perinatal clinical factors on postnatal brain developmental trajectories. Each factor was dichotomized using the clinically defined categorization ([Table 2](#)). To assess the association of the given clinical variable with T1w/T2w, MD, AD, RD, or FA values, we used a univariate mixed-effect linear model that addressed within-subject changes and intersubject effects. We tested difference in each imaging feature values between the 2 groups dichotomized for each clinical variable while correcting for PMA.

T1w/T2w and DTI measurements associated with clinical factors and neurodevelopmental outcomes

To probe whether cyto/myeloarchitectural maturation is associated with brain functional development, we examined whether T1w/T2w and DTI parameters at neonatal scan were associated with neurodevelopmental outcomes, i.e. the Bayley-III scores. Specifically, we employed general linear models (GLMs) to calculate the statistical association between T1w/T2w, MD, and FA values extracted from the midcortical and sWM surfaces from all 76 cortical regions and the neurodevelopmental outcome. The model controlled for sex, scan age, and clinical factors, including gestation age at birth, birth weight, VM

score, IVH score, WMI score, days of intubation, hypotension, infection, patent ductus arteriosus (PDA), necrotizing enterocolitis (NEC), and chronic lung disease (CLD). The false discovery rate was applied to control for multiple comparisons and adjust the *P* values. A significant difference was considered to be an adjusted *P* value ≤ 0.05 .

Results

Global trajectory of cyto/myeloarchitectural maturation

For T1w/T2w ratio developmental trajectory, the second-order polynomial model showed a better fitting (midcortical surface: $R = 0.443$; sWM surface: $R = 0.580$) than the linear model (mid: $R = 0.378$; superficial: $R = 0.542$). On the midcortical surface, the model showed that the global T1w/T2w ratio declined along with PMA increase until around 31–32 GW and started increasing after 32 GW ([Fig. 1](#)). In the same fashion, the T1w/T2w ratio sampled on the sWM surface declined until around 31–32 GW and increased thereafter.

For diffusion metrics, FA on the midcortical surface decreased linearly along with PMA increase ($R = -0.504$), whereas FA on sWM surface increased linearly ($R = 0.292$). In addition, MD sampled on the midcortical surface presented a linearly decreasing trajectory along with PMA increase ($R = -0.380$). For the sWM surface, MD also showed a negative linear relationship with PMA ($R = -0.559$). Similar patterns were observed in RD and AD measurements ([Supplementary Fig. S3](#)).

Spatiotemporal maturational trajectory

We fitted the second polynomial curve or the linear model to the individual data of each feature (T1/T2, MD, and FA) for each ROI separately. At each of the 4 different time points (28, 32, 36, and 40 weeks PMA), we then extracted each regional feature value from the fitted curve/line. These regional feature values of each T1w/T2w, FA, and MD at 28, 32, 36, and 40 GW are used to generate the temporally changing maps, as shown in [Fig. 2](#), respectively. For each feature, we also included the results of the *k*-mean clustering that labeled all 76 ROIs into either fast or slow maturation.

T1w/T2w ratio

All cortical regions showed a similar “U-shaped” parabolic developmental trajectory of T1w/T2w values, with a significant association with PMA at scan ($R > 0.44$; $P < 0.0001$). The inflection point of T1w/T2w values was found at around 32 GW for all regions consistently.

The spatiotemporal pattern of T1w/T2w changes on the midcortical surface across different PMA values is shown in [Fig. 2A](#), top. At 28 GW, ventral regions, including lateral occipitotemporal and orbitofrontal, temporal, and occipital cortices, showed relatively higher T1w/T2w values than dorsal regions, including the superior frontal, central, and parietal lobes. Around 32 GW, T1w/T2w

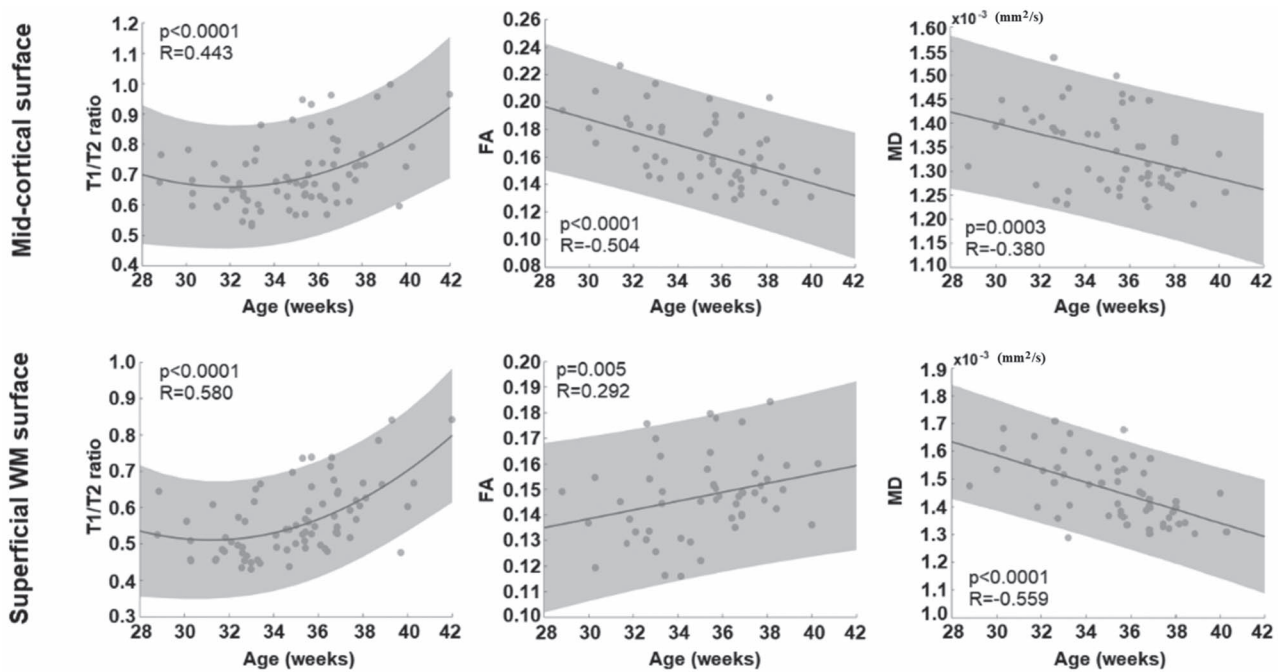


Fig. 1. Global trajectory of cyto/myeloarchitectural maturation. While the trajectory of T1/T2 ratio metric was best fitted by parabolic (=second-order polynomial) curve in both cortical GM and sWM, that of DTI-FA and MD metrics was linear. In GM, we found a decrease of FA along with PMA increase, whereas an increase was found in sWM. The MD value linearly decreases over time in both GM and sWM.

values decreased to the inflection point in all regions. The occipital area exhibited a slightly higher T1w/T2w ratio value than other regions. From 32 to 36 GW, T1w/T2w ratio increased globally, especially in central and superior temporal cortices. At 40 GW, central and ventral cortical areas showed much higher T1w/T2w values than other areas. Particularly, values in the medial occipital cortex were the highest among all ROIs. *k*-mean clustering showed that frontal, middle and inferior temporal, and lateral occipital cortices exhibit slow increases from 32 to 40 GW, whereas superior, while basal and medial temporal, orbitofrontal, central, and medial occipital cortical regions exhibit fast increases by 40 GW.

We also plotted the spatiotemporal pattern of T1w/T2w changes occurring in the sWM over different PMA (Fig. 2A, bottom). At 28 GW, ventral regions, especially the medial occipitotemporal area and para-hippocampus, presented slightly higher T1w/T2w values. By 32 GW, there were globally observed T1w/T2w decreases to the lower inflection in sWM. At 36 GW, the T1w/T2w ratio increased globally with more noticeable changes in the central, ventral, and temporal cortices. At 40 GW, all cortical regions displayed T1w/T2w increases than 32 and 36 GW. *k*-mean clustering showed fast increases in lateral orbitofrontal, central, superior, basal, and medial temporal regions.

DTI-FA

At 28 PMW, cortical FA values were higher in lateral frontal, lateral temporal, and lateral occipital cortical regions relative to that in primary sensorimotor areas (Fig. 2B, top). However, we found the opposite pattern

by 40 GW in which lateral frontal, temporal, and occipital regions showed rapidly decreased FA values by 40 GW, as also observed in the *k*-mean clustering result. By contrast, the central, cingulate, medial frontal, and orbitofrontal regions underwent relatively slow FA decreases by 40 GW.

The sWM anisotropy underwent more heterogeneous and more dynamic changes compare to the anisotropy changes in GM (Fig. 2B, bottom). FA values increased with PMA in sWM, but different regions had distinct developmental patterns. The cingulate region maintains a relatively high FA value throughout different PMAs. The frontal lobe, especially the superior frontal cortex, has the lowest FA value at 28 GW, but it reached a relatively high FA value by 40 GW compared to other sWM brain regions. Generally, dorsal (superior) areas have lower FA values (<0.13) than ventral (inferior) areas in the initial stage, but dorsal areas reached higher FA values (>0.16) than ventral areas at 40GW, especially in central, superior, and medial frontal regions. Ventral areas underwent moderate anisotropy changes with increasing PMA. Noticeably, the precuneus, cuneus, parahippocampal, and lateral occipitotemporal cortices displayed no FA changes or slight decreases as the PMA increased.

DTI-MD

In cortical GM (Fig. 2C, top), the lateral-dorsal cortical convexity, including lateral frontal, posterior cingulate, temporal, and parietal cortical areas, maintained lower and more rapidly decreasing MD values than other cortical regions throughout development. By contrast, the medial-ventral cortical regions, including olfactory,

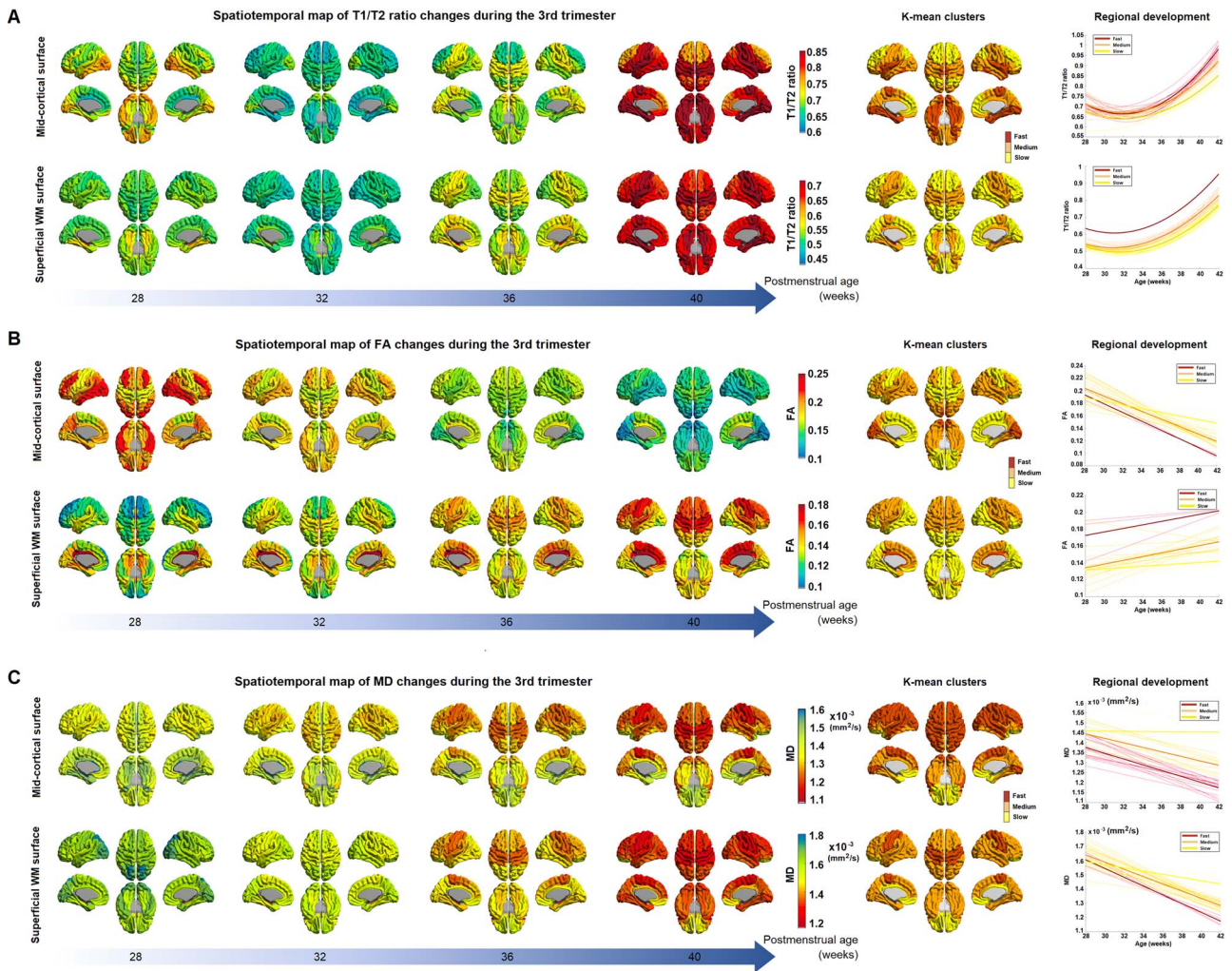


Fig. 2. Spatiotemporal map of T1w/T2w intensity ratio A), DTI-FA, B), and MD C) during the third trimester. A) The maps present T1w/T2w values on the second polynomial curve fitted into the preterm data at each vertex. Midcortical surface (top) and sWM surface (bottom) are shown. B and C) The maps present FA values on the linear model fitted into the preterm data at each vertex. The spatiotemporal pattern of each metric is mapped every 4 weeks from 28 to 40 weeks of PMA. The k-mean clustering results (the 2 most right columns) show 3 regions with fast, medium, and slow maturation along with their developmental trajectories.

basal/medial temporal, orbitofrontal, and cingulate cortices, presented higher and more slowly decreasing MD values.

In sWM (Fig. 2C, bottom), the degree of MD at each cortical area differed from that seen in cortical GM. However, the overall spatiotemporal pattern of sWM was similar to the changes of cortical GM. One particular observation was that at 28 GW, the occipital region displayed relatively higher MD value than other regions. By 36 GW, central and cingulate WM regions showed a more rapid decrease in MD (=faster sWM development) than other regions. By 40 GW, most areas except the orbitofrontal, middle/inferior temporal, and anterior cingulate WMs (>0.0013) reached a similar low MD value (0.0011–0.0013).

Feature correlation

T1w/T2w and DTI parameters may represent different aspects of cyto/myeloarchitectural maturation (Glasser and Van Essen 2011), while any 1 of these parameters may not fully explain all aspects of cortical maturation.

Particularly, the T1w/T2w ratio that has been used to explain the degree of cortical myelination in adult brains may also be affected by cytoarchitectural changes coinciding in the third trimester and early postnatal period, including selective elimination of neuronal processes through cell death and proliferation and differentiation of glia (Mrzljak et al. 1988). To understand the relationship between T1w/T2w and DTI parameters, we computed the correlation between T1w/T2w and DTI measurements for each cortical ROI (38 ROIs after merging the left and right hemispheres; Fig. 3).

In cortical GM, T1w/T2w ratio showed similar patterns in regional correlations with DTI-MD in which about half of cortical regions displayed negative correlations (17 ROIs [44%] with a large effect size of correlation coefficient $|r| \geq 0.5$) and only few showed positive correlations (3 ROIs [7%] with $r > 0.05$). By contrast, T1w/T2w ratio showed a mixture of positive and negative correlations with FA (7 ROIs [18%] with $r > 0.5$; 15 ROIs [39%] with $r < -0.5$). For example, T1w/T2w ratio in precentral,

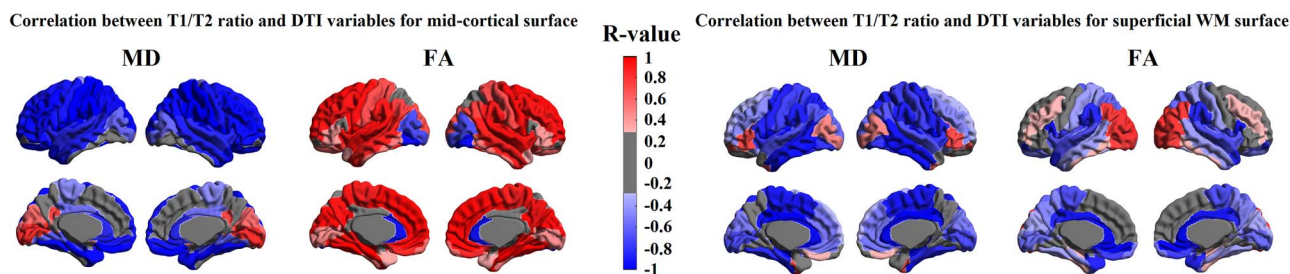


Fig. 3. Relationship between T1w/T2w intensity ratio and DTI-parameters. Colors represent either negative (blue), positive (red), or nonsignificant (gray) correlations between T1w/T2w intensity ratio and each DTI parameter, MD, and FA.

parahippocampal, angular, and inferior temporal regions correlated positively with FA but negatively with diffusivity. Contrarily, T1w/T2w values in orbital, inferior frontal, superior occipital, and temporal pole regions correlated negatively with FA but positively with diffusivity metrics. In superior temporal, cingulate, supramarginal gyrus, central lobular, precuneus, and cuneus regions, T1w/T2w ratio correlated negatively with both diffusivity metrics and FA. In the middle occipital gyrus, T1w/T2w ratio correlated positively with both diffusivity metrics and FA (Fig. 3).

In sWM, T1w/T2w ratio negatively correlated with diffusivity metrics (MD) in the majority of regions (27 ROIs [71%] with $r < -0.5$). Only the posterior cingulate, cuneus, and olfactory cortices showed significant positive correlations between T1w/T2w and diffusivity metrics (3 ROIs [7%] with $r > 0.5$). By contrast, T1w/T2w ratio positively correlated with FA in most regions (30 ROIs [79%] with $r > 0.5$). The lateral occipital, cingulate, and orbitofrontal cortices showed negative correlations with FA (3 ROIs [7%] with $r < -0.5$) (Fig. 3). Similar analyses on AD and RD can be found in [Supplementary Fig. S4](#).

The association between clinical factors and imaging features of cortical development

Our univariate analyses showed that severe brain injury (IVH) was related to increased diffusivity in both cortical GM (parahippocampal cortex) and sWM (parahippocampal and lingual cortices) because the severely injured group presented a higher MD value than the unaffected group (Fig. 4). The sWM showed more pronounced and extended damage in relation to severe brain injury compared to GM.

Cognitive score association

Our GLM analysis showed that T1w/T2w was significantly associated with cognitive and language scores at 12 months in most regions of the midcortical surface ($t > 3.1$; $P < 0.05$). Particularly, frontal cortical regions showed the most significant associations with cognitive scores. On the other hand, Broca's area and the temporal cortex showed the most significant association with language scores (Fig. 5). On the sWM surface, we found similar patterns, where the frontal cortex showed a significant association with cognitive scores; Broca's area and the temporal cortex showed a significant association

with language scores (Fig. 5). No cortical regions were significantly associated with motor scores at 12 months. Important features relative to cognitive performance at 12 months largely overlapped with those relative to language function. This is possibly because subjects showed a significant correlation between their cognitive and language functional scores ($r = 0.63$).

DTI parameters for either midcortical or sWM surfaces showed no significant associations with neurodevelopmental outcomes ($P > 0.1$). In addition, midcortical and sWM imaging features did not correlate with neurodevelopmental outcomes measured at 18 and 30 months.

Developmental trajectory of WM tracts

To better elucidate the relationship between T1/T2 ratio and DTI variables in the deep/core WM regions, we further conducted a WM tractography analysis. We extracted the 10 important WM tracts labeled on the John-Hopkins's WM atlas that was registered into our age-specific neonatal brain templates and analyzed the T1/T2 ratio and all DTI parameters in association with PMA at scan for all these WM tracts.

Overall results (Fig. 6) exhibited that T1/T2 ratio increased and that DTI-diffusive parameters (MD) decreased along with PMA increases, which was similar to the trends in our analysis of sWM. More specifically, T1/T2 ratio for all 10 tracts positively correlated with the PMA at scan. DTI-MD significantly negatively correlated with PMA at scan in most of the tracts (including anterior thalamic radiations, corticospinal tract, cingulum-cingulate gyrus bundle, cingulum of the hippocampal region [CGH], uncinate fasciculus [UF], and superior longitudinal fasciculus-temporal endings; corpus callosum-forceps). Finally, we found a mixed pattern of regional FA increases (CGH and inferior longitudinal fasciculus) and decreases (UF) along with increasing PMA. The analyses of AD and RD can be found in [Supplementary Fig. S5](#).

Discussion

Summary of findings

Our study revealed differential developmental trajectories of global T1w/T2w as well as DTI FA and MD across the cerebral cortex in both cortical GM and sWM, indicating that the microstructural properties inferred

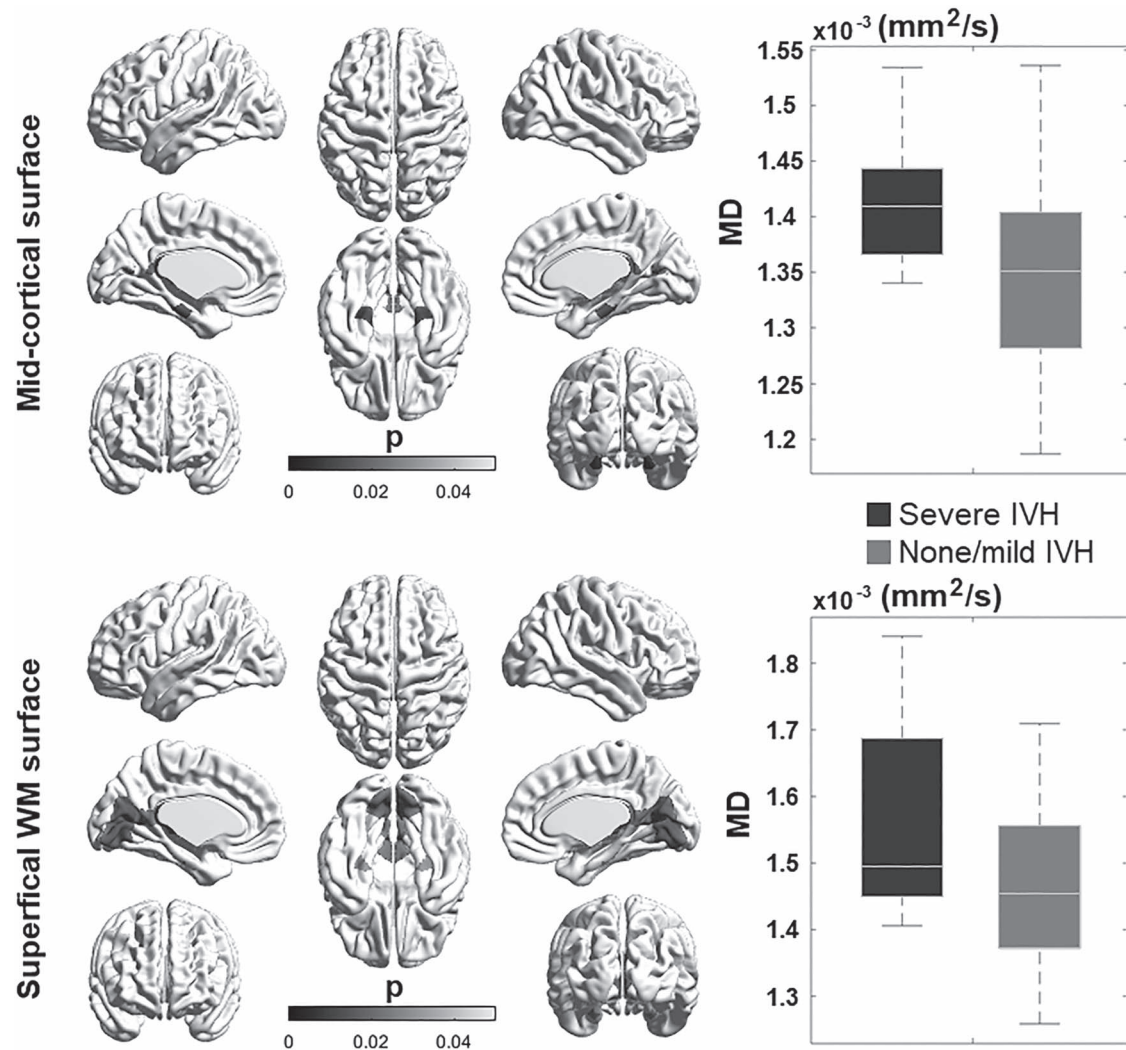


Fig. 4. The effect of perinatal brain injury and postnatal clinical factors on cortical GM and sWM maturation in preterm neonates. The presence of severe IVH is associated with higher MD in GM and WM regions.

by the 2 measurements are distinct (Fig. 1). Furthermore, the microstructural developmental courses of T1w/T2w and DTI parameters were found to be regionally varying across the cerebral cortex, suggesting their sensitivity and specificity to important local cyto/myeloarchitectural changes (Figs 2 and 3). Finally, T1w/T2w and DTI-FA were significantly associated with neurodevelopmental outcomes and clinical conditions, demonstrating their potential in quantifying aberrant neurodevelopment (Figs 4 and 5).

Developmental trajectory of cortical GM and associated cyto/myeloarchitectural processes

Our results showed that global FA values decrease in cortical GM throughout the third trimester (Fig. 1). Decreasing global FA in cortical GM is largely consistent with previous findings (McKinstry et al. 2002; Smyser et al. 2016) and has been interpreted as due to the lack of diffusion barriers upon radial glia apoptosis (Ouyang, Jeon, et al. 2019). The higher anisotropy in early developing

cortical GM may also be due to the predominance of radial glial fibers (RGF), or neurons with simple axons and an underdeveloped dendritic tree, while the decline over the period from 26 to 40 weeks may reflect the expansion of dendritic tree and axonal ramifications alongside the regression of RGFs. Accordingly, 1 recent study using DTI metrics proposed a hypothetical model in which cortical FA values are predominantly influenced by RGF apoptosis (Ouyang, Jeon, et al. 2019).

In contrast to FA trends, we found a distinct parabolic trend of T1w/T2w values in cortical GM (Fig. 1), which may capture more subtle cyto/myeloarchitectural changes. Specifically, we found that T1w/T2w values decrease from 28 to 32 weeks but increase parabolically from 32 to 40 weeks. The initial T1w/T2w decreases between 28 and 32 weeks may be principally driven by radial glial cell organization, whereas cyto/myeloarchitectural events may predominate to drive T1w/T2w increases between 32 and 40 weeks as the radial cells undergo apoptosis and differentiate into neuronal

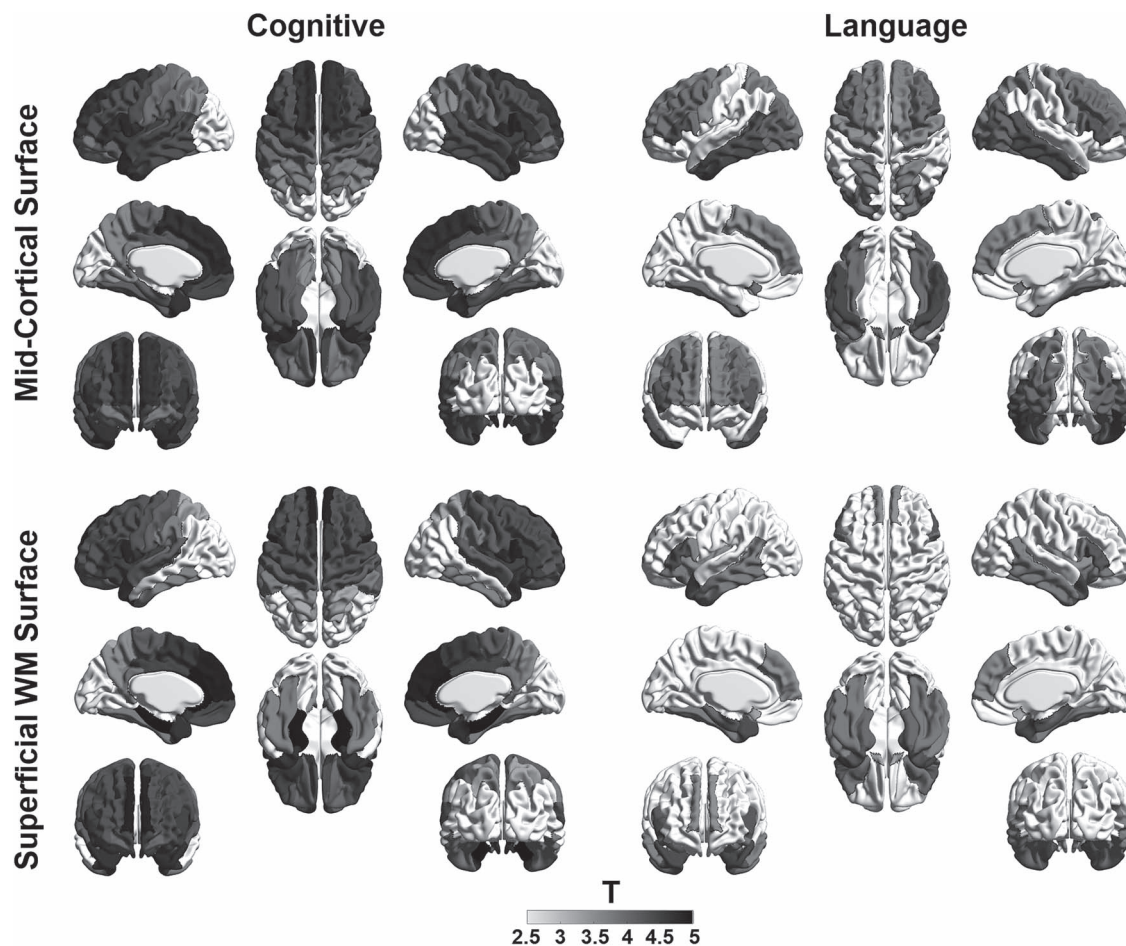


Fig. 5. The association of neurodevelopmental outcomes and cortical GM and sWM maturation in preterm neonates. GLM showed that T1w/T2w ratio was significantly associated with cognitive and language scores at 12 months in most cortical regions of the midcortical surface. Particularly, frontal cortical regions showed the most significant association with cognitive scores (left). On the other hand, Broca's area and the temporal cortex showed the most significant association with language scores (right).

precursors. In fact, several studies have already proposed that T1w/T2w is not only sensitive to intracortical myelination properties (Glasser and Van Essen 2011; Shafee et al. 2015) but also to cortical dendrite pathology (Arshad et al. 2017; Righart et al. 2017; Petracca et al. 2020). It is also important to note that there is relatively little cortical myelin in the preterm age range. Thus, T1w/T2w increases may reflect a variety of cyto/myeloarchitectural changes, including the elaboration of dendritic and axonal ramifications, establishment of synaptic contacts, selective elimination of neuronal processes through cell death, and proliferation and differentiation of glia (Mrzljak et al. 1988).

Developmental trajectory of sWM and associated cyto/myeloarchitectural processes

Our findings revealed that the developmental trajectory of FA values in sWM is different from that of cortical GM, indicating differential developmental roles of the 2 tissue subtypes despite their close proximity. Specifically, we found that FA values linearly increased in sWM, which was consistent with prior studies reporting marked

increases in WM FA from the third trimester to 1 years old, followed by more subtle increases from 1 to 2 years old (Huppi et al. 1998; Gao et al. 2009; Geng et al. 2012; Smyser et al. 2016; Wilson et al. 2021). Our findings on linear FA developmental trends in sWM are also consistent with studies that observed similar linear trends in deep WM tracts (Bui et al. 2006; Keunen et al. 2018; Khan et al. 2019; Jaimes et al. 2020) but contrast a more recent study that found distinct developmental ontogenies of specific WM tracts with several showing nonlinear changes in tract microstructure during second and third trimesters (Wilson et al. 2021). Notably, the in utero study by Wilson et al. (2021) reported complex nonlinear trends in WM tracts of fetuses with an initial decrease in FA in early brain development before 30–32 weeks of gestation followed by a later increase, which is similar to our study's nonlinear T1w/T2w ratio trends in preterm neonates. Further studies are needed to better characterize the differences between in utero and ex utero brain development during this time period. However, it is important to note that, in contrast to deep WM tracts that play an important role

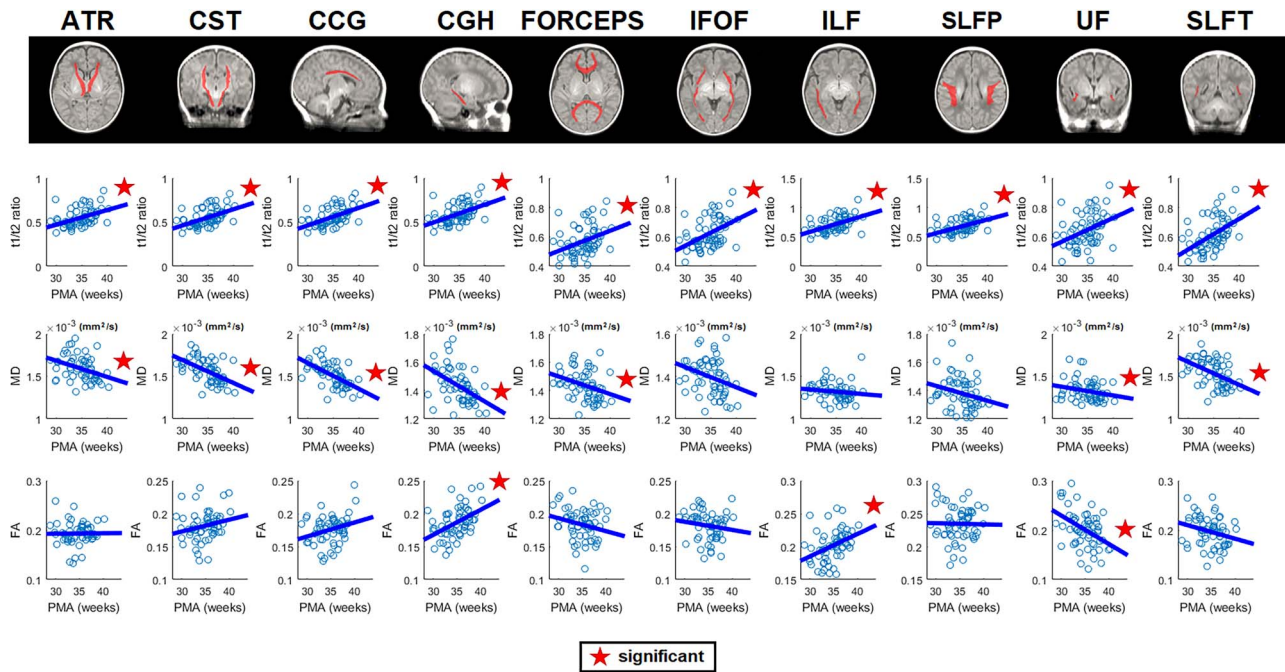


Fig. 6. Axonal maturation on major WM tracts. Top: 10 ROI WM tracts labeled on the Johns-Hopkins' WM atlas that was registered into our age-specific neonatal brain templates. Bottom: Maturation trajectory in preterm neonates: the T1/T2 ratio and all DTI parameters in association with PMA at scan for each WM tract. Overall results showed that the T1/T2 ratio increased and that DTI-diffusive parameters (MD) decreased along with increasing PMA, which is similar to the sWM trends in our analysis. We also found a mixed pattern of regional FA increases (CGH and ILF) and decreases (UF) along with increasing PMA. (Abbreviations: ATR = anterior thalamic radiations; CST = corticospinal tract; CCG = cingulum-cingulate gyrus bundle; FORCEPS = corpus callosum-forceps; IFOF: inferior fronto-occipital fasciculus; ILF = inferior longitudinal fasciculus; SLFP = superior longitudinal fasciculus-parietal endings; SLFT = superior longitudinal fasciculus-temporal endings.).

in subcortical and remote cortical connectivity, sWM is strongly influenced by cortical GM, particularly short cortical association fibers (also called arcuate or “U”-fibers), which connect adjacent gyri and comprise the majority of corticocortical WM connections (Kirilina et al. 2020). Thus, FA increases in sWM may indicate stronger influence from axonal packing organization and myelination on short corticocortical WM connections.

This is further supported by our findings on a less parabolic and more linear trajectory of T1w/T2w in sWM, implicating the expansion of myeloarchitectural events. Throughout development, myelination events occur through the oligodendroglial lineage that begins with the oligodendroglial progenitor and continues successively with the preoligodendrocyte, the immature oligodendrocyte, and the mature oligodendrocyte. In early third trimester, preoligodendrocyte differentiate into immature oligodendrocyte predominate. And during the later stage of the third trimester, axonal ensheathment by premyelinating oligodendrocytes predominate (Back et al. 2001, 2002), contributing to premyelination anisotropy (Wimberger et al. 1995; Drobyshevsky et al. 2005) and increases in T1w/T2w intensity (Glasser and Van Essen 2011).

Our exploration of the relationship between T1w/T2w and FA (Fig. 3) showed that while T1w/T2w values were mostly negatively correlated with FA in cortical GM, they were significantly positively correlated with FA in sWM. This supports our aforementioned hypothesis that

information inferred by T1w/T2w values in cortical GM is different from that inferred by FA and is consistent with prior multiparametric studies reporting that each parameter differently reflects the cortical microstructure (Lebenberg et al. 2019; Fenchel et al. 2020). More specifically, a negative correlation between T1w/T2w and FA in cortical GM regions supports our hypothesis that cerebral cortical GM undergoes combined cyto/myeloproliferative events beyond simplified events related to radial glial cell apoptosis. By contrast, a positive correlation between T1w/T2w and FA in sWM confirms that myeloproliferative information inferred by both FA and T1w/T2w may overlap in sWM. Although T1w/T2w ratios have been shown to be sensitive to myelin in only the cortex and less so in WM of healthy adults (Glasser and Van Essen 2011), it is possible that T1w/T2w values encompass myeloproliferative events in sWM just underneath the cortical sheet. However, further studies are needed to more accurately define the microstructural properties driving these measurements. It will also be important to explore methods that integrate these varied metrics for comprehensive cortical profiles that globally depict the highly dynamic processes during this critical period (Lebenberg et al. 2019; Fenchel et al. 2020).

Consistent decreases in MD for cortical GM and adjacent sWM

Our findings demonstrate that global MD values decrease in both cortical GM and sWM throughout the third

trimester. Several developmental studies have found similar trends in WM where decreasing MD is coupled with a rise in FA in preterm infants (Miller et al. 2002; Partridge et al. 2004; Bava et al. 2010; de Bruine et al. 2011; Kersbergen et al. 2014), term infants (Dubois et al. 2006; Gao et al. 2009; Oishi et al. 2011; Geng et al. 2012), and adolescence (Lobel et al. 2009; Schmithorst and Yuan 2010). In an intriguing contrast, cortical GM exhibits overall decreases in both MD and FA, as shown in prior studies on preterm subjects (McKinstry et al. 2002; Smyser et al. 2016). Decreasing MD in GM can be reflective of more complex microstructural barriers to diffusion due to cyto/myeloproliferative events. These changes may be explained by decreasing diffusivity of the radial direction (RD; Supplementary Fig. S3), implicating stronger influence of myelination events and formation of new barriers in this process (Song et al. 2003, 2005; Budde et al. 2007; Gao et al. 2009). Indeed, it is well established that myelination events progress throughout the third trimester, adolescence, and up to adulthood where these changes plateau (Volpe 1981).

Heterogeneous spatiotemporal patterns of cortical and sWM T1w/T2w and DTI-FA and MD measurements

Our results suggest that T1w/T2w and DTI-FA and MD developmental trajectories are unique and differential across cortical regions. Such heterogeneous developmental profiles possibly lead to unique cortical regions important for distinct neural circuitry, tract-specific maturational trends, and functional systems (Huttenlocher and Dabholkar 1997; Canini et al. 2020; Edde et al. 2021; Wilson et al. 2021) and that 1 metric alone cannot fully differentiate the components of WM microstructural maturation (Gao et al. 2009; Lebenberg et al. 2019; Fenchel et al. 2020). Among these patterns, one noteworthy finding is that FA decreased more rapidly in the frontal, temporal, and occipital cortical GM areas by the 40th week of gestation, indicating that these regions underwent more intense cytoarchitectural changes throughout development. By contrast, slower FA decreases in the central, cingulate, and medial frontal regions suggest that they undergo maturation even earlier. Relatively low FA values at 30 weeks with slower decrease thereafter in the primary sensorimotor cortex also suggest its earlier development compared to higher-order prefrontal cortical regions, as the folding of sensorimotor cortices is most active during the late second and early third trimester before 30 weeks (Wright et al. 2014; Kim, Lepage, et al. 2016). Altogether, these regionally specific changes demonstrate a developmental gradient moving along a caudal to rostral direction with primary somatosensory cortices developing earliest and prefrontal and association areas later, which is consistent with patterns documented in prior postmortem histopathological findings (Volpe 1981) and myelin staining (Flechsig Of Leipsic 1901; Flechsig 1920) as well as the heterogeneity of FA decreases

observed in prior DTI studies (Deipolyi et al. 2005; Gao et al. 2009; Ball et al. 2013; Yu et al. 2016).

Spatiotemporally, MD values decreased the slowest in the lateral cortical convexity of both sWM and GM, including lateral frontal, temporal, and parietal regions, indicating their faster maturation of cortical premyelinated axons relative to other regions. Paralleling what has been observed in prior studies (Kinney et al. 1988, 1994), these regional variations in the timing of this developmental trajectory follow a roughly posterior-to-anterior trend.

Cortical T1w/T2w and DTI measurements associated with neurodevelopmental outcome and clinical characteristics

Importantly, our study also found that T1w/T2w and FA correlated neurodevelopmental assessment scores for cognitive and language functions measured at 12 months. MD did not significantly correlate with outcomes in preterm neonates potentially due to its informational redundancy as it positively and strongly correlated with T1w/T2w. Brain regions that correlated with cognitive scores included the medial frontal cortex and cingulate, which are important for learning, decision-making, and memory. Language scores were also correlated with the corresponding region of the superior temporal lobe, which is involved in the comprehension of language. These findings confirm that myelin maturational processes are associated with the development of cognitive domains during the human life span and represent the anatomic correlate of neurophysiological maturation (Geng et al. 2012). Interestingly, features that correlated with cognitive performance at 12 months largely overlapped with those that correlated with language function, indicating the widespread involvement of cortical regions in establishing synaptic architecture for multiple domains in early neurodevelopment. Our findings on the significant correlation between cognitive and language scores at 12 months also support the notion that multiple cortical regions may synchronize into a network of domains, as prior findings have indicated the formation of functional and structural networks throughout preterm development (van den Heuvel et al. 2015). However, our models that were separately applied to each correlation of either cognitive or language function did not account for the covariance of these 2 functions, limiting the specificity of imaging features to different functional domains. Importantly, the significant correlation of language and cognitive scores using neonatal cyto/myeloarchitectural features was only found in the early 12 months of infancy but not for later years i.e. 24–30 months. This implicates that impairments in cyto/myeloarchitectural maturations may recover as these processes continue throughout adolescence and thus may not be as sensitive to long-term neurodevelopmental outcomes. By contrast, other features of neonatal brain MRI, such as connectivity or morphological alterations, i.e. cortical folding, may

be more permanent and significantly associated with long-term impairments as supported in previous studies (Kawahara et al. 2017; Gui et al. 2019).

Additionally, our analyses demonstrated that severe IVH is associated with increased diffusivity in both cortical GM (parahippocampal cortex) and sWM (parahippocampal and lingual cortices) (Fig. 4), suggesting that IVH may impede regionally specific microstructural maturation. These findings align with prior studies suggesting that medical risk factors, including IVH, may be an important predictor of poor neurologic outcome.

Altogether, these findings are consistent with prior findings reporting that regionally specific cortical architecture in early development underlies brain function in adolescent years and serves as a potential biomarker in relation to future neurodevelopmental outcomes (Smyser et al. 2016).

Limitations and future directions

Our study has several limitations. Specifically, our ability to fully characterize cortical cyto/myeloarchitectural development was limited by a small sample size of 78 neonates in which not every subject had a successful follow-up scan. Thus, this study is limited by its partial longitudinal design despite its mixed-effect models for statistical analyses. Additionally, this study analyzed only preterm neonates, which may have impacted our ability to assess normal development, as preterm birth itself may alter brain development even after correcting for PMA at birth. Due to a small sample size, the effects of the related risk factors, including variables listed in Table 1, were analyzed only in a univariate fashion without adjusting for their combined effects. Furthermore, our interpretation is limited to the third trimester of development, as data points above 38 weeks are lacking, leading to residual uncertainty on the particular cytologic features after term age and beyond. Nevertheless, our study contributes to the growing body of research that leverages MRI to examine preterm cortical development throughout the third trimester (McKinstry et al. 2002; Ball et al. 2013; Ouyang, Dubois, et al. 2019).

Another technical limitation of this paper is the identification of the very thin cortical ribbon at this age, which makes the registration-projection of DTI maps (with a DTI slice thickness of 3 mm) onto T1w anatomical images challenging. Certainly, the accuracy of coregistration between T1w and DTI data and the partial volume effects due to the relatively low spatial resolution are important issues to ensuring reliable and biologically meaningful measurements. To overcome these issues, our study obtained the cortical ribbon using our recent segmentation and surface reconstruction methods (Liu et al. 2020, 2021) that have been systematically and comprehensively validated using multisite datasets. To perform an accurate coregistration, we took advantage of the intensity similarity between T2w and b0 MR images while using a diffeomorphic mapping method

(implemented in ANTs software) to nonlinearly warp the b0 images to T2 images within each individual. The distortion of DTI maps was addressed partially through this nonlinear warping along with the FSL-eddy current correction that was applied in the DTI preprocessing. Based on the estimated transformation parameters in the rigid registration between T2w and T1w images, each b0 volume (together with MD/AD/RD and FA volumes) was further transformed to the same individual's T1w image for mapping the diffusion data on midcortical and sWM surfaces. The registration results are exemplified in Supplementary Fig. S1 presenting individually paired T1w and DTI-FA maps at different ages. To avoid partial volume effects, we then sampled GM-DTI parameters on the midcortical surface (=surface generated by averaging each of the paired vertices placed on GM/WM and GM/CSF surfaces) and WM-DTI parameters on the sWM surface generated by deforming GM/WM surface inwardly 2 mm in depth via the surface normal direction. Nevertheless, our measurement could not fully address partial volume effects due to the relatively larger size of voxels compared to cortical thickness ($1.56 \times 1.56 \times 3$ mm vs. approximately 1–1.5 mm in preterm neonates).

Finally, although our innovative approach in combining T1w/T2w and DTI parameters effectively characterized the dynamics of cortical development, the proposed cyto/myeloarchitectural models and its clinical utility require future studies to validate with neurohistological measurements, including neuronal density, glial proliferation, or dendritic arborization.

Conclusion

Overall, with noninvasive properties of cortical T1w/T2w and DTI-FA and MD measurements, this study provides an innovative approach to the longitudinal spatiotemporal mapping of cortical cyto/myeloarchitecture, offering unique insights into the cellular processes and associated developmental mechanisms during the third trimester. T1w/T2w measurements complement DTI-derived FA measurements through its unique parabolic trend encompassing the timing of cyto/myeloarchitectural events, including radial glial cell organization and apoptosis, dendritic arborization, myelination, synaptic formation, and potentially brain circuit emergence. While the exact neuroanatomical underpinning of cortical T1w/T2w and DTI metrics in cortical GM and its adjacent sWM is not completely known, the unique combination of DTI linear trajectories and T1w/T2w parabolic trajectories contribute new insights on cyto/myeloarchitectural events in brain development. And finally, our study demonstrates that DTI and T1w/T2w measurements of microstructural cortical signature are sensitive to impacts from clinically adverse events and may serve as early imaging biomarkers of future neurodevelopmental outcome.

Supplementary material

Supplementary material is available at *Cerebral Cortex Journal* online.

Funding

This study was supported by the National Institutes of Health grants (P50NS035902, P01NS082330, R01NS046432, R01HD072074, P41EB015922, U54EB020406, U19AG024904, U01NS086090, 003585-00001) and BrightFocus Foundation Award (A2019052S).

Data Availability

All data used in this study will be made available on request from any qualified investigator who provides a practicable proposal, or for the purpose of replicating procedures and results presented in the current study.

Conflict of interest statement. None declared.

References

- Akaike H. Citation classic—a new look at the statistical-model identification. *Cc/Eng Tech Appl Sci*. 1981;51:22–22.
- Anjari M, Srinivasan L, Allsop JM, Hajnal JV, Rutherford MA, Edwards AD, Counsell SJ. Diffusion tensor imaging with tract-based spatial statistics reveals local white matter abnormalities in preterm infants. *NeuroImage*. 2007;35:1021–1027.
- Arshad M, Stanley JA, Raz N. Test-retest reliability and concurrent validity of in vivo myelin content indices: myelin water fraction and calibrated T1 w/T2 w image ratio. *Hum Brain Mapp*. 2017;38:1780–1790.
- Back SA, Luo NL, Borenstein NS, Levine JM, Volpe JJ, Kinney HC. Late oligodendrocyte progenitors coincide with the developmental window of vulnerability for human perinatal white matter injury. *J Neurosci*. 2001;21:1302–1312.
- Back SA, Luo NL, Borenstein NS, Volpe JJ, Kinney HC. Arrested oligodendrocyte lineage progression during human cerebral white matter development: dissociation between the timing of progenitor differentiation and myelinogenesis. *J Neuropathol Exp Neurol*. 2002;61:197–211.
- Ball G, Srinivasan L, Aljabar P, Counsell SJ, Durighel G, Hajnal JV, Rutherford MA, Edwards AD. Development of cortical microstructure in the preterm human brain. *Proc Natl Acad Sci U S A*. 2013;110:9541–9546.
- Barkovich AJ. Magnetic resonance techniques in the assessment of myelin and myelination. *J Inherit Metab Dis*. 2005;28:311–343.
- Batalle D, O’Muircheartaigh J, Makropoulos A, Kelly CJ, Dimitrova R, Hughes EJ, Hajnal JV, Zhang H, Alexander DC, Edwards AD. Different patterns of cortical maturation before and after 38 weeks gestational age demonstrated by diffusion MRI in vivo. *NeuroImage*. 2019;185:764–775.
- Bava S, Thayer R, Jacobus J, Ward M, Jernigan TL, Tapert SF. Longitudinal characterization of white matter maturation during adolescence. *Brain Res*. 2010;1327:38–46.
- Beaulieu C. The biological basis of diffusion anisotropy. In: *Diffusion MRI*. 2nd ed. Academic Press; 2014. pp. 155–183.
- Brody BA, Kinney HC, Kloman AS, Gilles FH. Sequence of central nervous system myelination in human infancy. I. an autopsy study of myelination. *J Neuropathol Exp Neurol*. 1987;46:283–301.
- Budde MD, Kim JH, Liang HF, Schmidt RE, Russell JH, Cross AH, Song SK. Toward accurate diagnosis of white matter pathology using diffusion tensor imaging. *Magn Reson Med*. 2007;57:688–695.
- Bui T, Daire J-L, Chalard F, Zaccaria I, Alberti C, Elmaleh M, Garel C, Luton D, Blanc N, Sebag G. Microstructural development of human brain assessed in utero by diffusion tensor imaging. *Pediatr Radiol*. 2006;36:1133–1140.
- Canini M, Cavoretto P, Scifo P, Pozzoni M, Petrini A, Iadana A, Pontesilli S, Scotti R, Candiani M, Falini A, et al. Subcortico-cortical functional connectivity in the fetal brain: a cognitive development blueprint. *Cerebral Cortex Commun*. 2020:1.
- Chao LL, Tosun D, Woodward SH, Kaufer D, Neylan TC. Preliminary evidence of increased hippocampal myelin content in veterans with posttraumatic stress disorder. *Front Behav Neurosci*. 2015;9:333.
- Chen H, Budin F, Noel J, Prieto JC, Gilmore J, Rasmussen J, Wadhwa PD, Entringer S, Buss C, Styner M. White matter fiber-based analysis of T1w/T2w ratio map. *Proc SPIE Int Soc Optim Eng*. 2017:10133.
- Chopra S, Shaw M, Shaw T, Sachdev PS, Anstey KJ, Cherbuin N. More highly myelinated white matter tracts are associated with faster processing speed in healthy adults. *NeuroImage*. 2018;171:332–340.
- Clark VP, Courchesne E, Grafe M. In vivo myeloarchitectonic analysis of human striate and extrastriate cortex using magnetic resonance imaging. *Cereb Cortex*. 1992;2:417–424.
- Counsell SJ, Maalouf EF, Fletcher AM, Duggan P, Battin M, Lewis HJ, Herlihy AH, Edwards AD, Bydder GM, Rutherford MA. MR imaging assessment of myelination in the very preterm brain. *Am J Neuroradiol*. 2002;23:872–881.
- Counsell SJ, Edwards AD, Chew AT, Anjari M, Dyet LE, Srinivasan L, Boardman JP, Allsop JM, Hajnal JV, Rutherford MA, et al. Specific relations between neurodevelopmental abilities and white matter microstructure in children born preterm. *Brain*. 2008;131:3201–3208.
- de Bruine FT, van Wezel-Meijler G, Leijser LM, van den Berg-Huysmans AA, van Steenis A, van Buchem MA, van der Grond J. Tractography of developing white matter of the internal capsule and corpus callosum in very preterm infants. *Eur Radiol*. 2011;21:538–547.
- Deipolyi AR, Mukherjee P, Gill K, Henry RG, Partridge SC, Veeraghavan S, Jin H, Lu Y, Miller SP, Ferriero DM, et al. Comparing microstructural and macrostructural development of the cerebral cortex in premature newborns: diffusion tensor imaging versus cortical gyration. *NeuroImage*. 2005;27:579–586.
- Deoni SC, Dean DC 3rd, Remer J, Dirks H, O’Muircheartaigh J. Cortical maturation and myelination in healthy toddlers and young children. *NeuroImage*. 2015;115:147–161.
- Drobyshevsky A, Song SK, Gamkrelidze G, Wyrwicz AM, Derrick M, Meng F, Li L, Ji X, Trommer B, Beardsley DJ, et al. Developmental changes in diffusion anisotropy coincide with immature oligodendrocyte progression and maturation of compound action potential. *J Neurosci*. 2005;25:5988–5997.
- Dubois J, Hertz-Pannier L, Dehaene-Lambertz G, Cointepas Y, Le Bihan D. Assessment of the early organization and maturation of infants’ cerebral white matter fiber bundles: a feasibility study using quantitative diffusion tensor imaging and tractography. *NeuroImage*. 2006;30:1121–1132.
- Duerden EG, Foong J, Chau V, Branson H, Poskitt KJ, Grunau RE, Synnes A, Zwicker JG, Miller SP. Tract-based spatial statistics in preterm-born neonates predicts cognitive and motor

- outcomes at 18 months. *AJNR Am J Neuroradiol.* 2015;36:1565–1571.
- Ecker C, Stahl D, Daly E, Johnston P, Thomson A, Murphy DG. Is there a common underlying mechanism for age-related decline in cortical thickness? *Neuroreport.* 2009;20:1155–1160.
- Edde M, Leroux G, Altena E, Chanraud S. Functional brain connectivity changes across the human life span: from fetal development to old age. *J Neurosci Res.* 2021;99:236–262.
- Fenchel D, Dimitrova R, Seidlitz J, Robinson EC, Bataille D, Hutter J, Christiaens D, Pietsch M, Brandon J, Hughes EJ. Development of microstructural and morphological cortical profiles in the neonatal brain. *Cereb Cortex.* 2020;30:5767–5779.
- Flechsig P. *Anatomie des menschlichen Gehirns und Rückenmarks auf myelogenetischer Grundlage.* 1920 (Vol. 1). G. Thieme.
- Flechsig P, Leisic P. Developmental (MYELOGENETIC) localisation of the cerebral cortex in the human subject. *Lancet.* 1901;158:1027–1030.
- Gao W, Lin W, Chen Y, Gerig G, Smith J, Jewells V, Gilmore J. Temporal and spatial development of axonal maturation and myelination of white matter in the developing brain. *Am J Neuroradiol.* 2009;30:290–296.
- Geng X, Gouttard S, Sharma A, Gu H, Styner M, Lin W, Gerig G, Gilmore JH. Quantitative tract-based white matter development from birth to age 2 years. *NeuroImage.* 2012;61:542–557.
- Glasser MF, Van Essen DC. Mapping human cortical areas in vivo based on myelin content as revealed by T1- and T2-weighted MRI. *J Neurosci.* 2011;31:11597–11616.
- Glasser MF, Goyal MS, Preuss TM, Raichle ME, Van Essen DC. Trends and properties of human cerebral cortex: correlations with cortical myelin content. *NeuroImage.* 2014;93(Pt 2):165–175.
- Grydeland H, Walhovd KB, Tamnes CK, Westlye LT, Fjell AM. Intracortical myelin links with performance variability across the human lifespan: results from T1- and T2-weighted MRI myelin mapping and diffusion tensor imaging. *J Neurosci.* 2013;33:18618–18630.
- Gui L, Loukas S, Lazeyras F, Huppi PS, Meskaldji DE, Borradori TC. Longitudinal study of neonatal brain tissue volumes in preterm infants and their ability to predict neurodevelopmental outcome. *NeuroImage.* 2019;185:728–741.
- Halkidi M, Vazirgiannis M, Batistakis Y. Quality scheme assessment in the clustering process. *Lect Notes Comput & D.* 2000;1910:265–276.
- Hinojosa-Rodriguez M, Harmony T, Carrillo-Prado C, Van Horn JD, Irimia A, Torgerson C, Jacokes Z. Clinical neuroimaging in the preterm infant: diagnosis and prognosis. *Neuroimage Clin.* 2017;16:355–368.
- Huppi PS, Maier SE, Peled S, Zientara GP, Barnes PD, Jolesz FA, Volpe JJ. Microstructural development of human newborn cerebral white matter assessed in vivo by diffusion tensor magnetic resonance imaging. *Pediatr Res.* 1998;44:584–590.
- Huttenlocher PR, Dabholkar AS. Regional differences in synaptogenesis in human cerebral cortex. *J Comp Neurol.* 1997;387:167–178.
- Inder TE, Warfield SK, Wang H, Huppi PS, Volpe JJ. Abnormal cerebral structure is present at term in premature infants. *Pediatrics.* 2005;115:286–294.
- Iwatani J, Ishida T, Donishi T, Ukai S, Shinosaki K, Terada M, Kaneoke Y. Use of T1-weighted/T2-weighted magnetic resonance ratio images to elucidate changes in the schizophrenic brain. *Brain Behav.* 2015;5:e00399.
- Jaimes C, Machado-Rivas F, Afacan O, Khan S, Marami B, Ortinau CM, Rollins CK, Velasco-Annis C, Warfield SK, Gholipour A. In vivo characterization of emerging white matter microstructure in the fetal brain in the third trimester. *Hum Brain Mapp.* 2020;41:3177–3185.
- Kawahara J, Brown CJ, Miller SP, Booth BG, Chau V, Grunau RE, Zwicker JG, Hamarneh G. BrainNetCNN: convolutional neural networks for brain networks; towards predicting neurodevelopment. *NeuroImage.* 2017;146:1038–1049.
- Kersbergen KJ, Leemans A, Groenendaal F, van der Aa NE, Viergever MA, de Vries LS, Benders M. Microstructural brain development between 30 and 40 weeks corrected age in a longitudinal cohort of extremely preterm infants. *NeuroImage.* 2014;103:214–224.
- Keunen K, van der Burgh HK, de Reus MA, Moeskops P, Schmidt R, Stolwijk LJ, de Lange SC, Išgum I, de Vries LS, Benders MJ. Early human brain development: insights into macroscale connectome wiring. *Pediatr Res.* 2018;84:829–836.
- Khan S, Vasung L, Marami B, Rollins CK, Afacan O, Ortinau CM, Yang E, Warfield SK, Gholipour A. Fetal brain growth portrayed by a spatiotemporal diffusion tensor MRI atlas computed from in utero images. *NeuroImage.* 2019;185:593–608.
- Kim H, Lepage C, Maheshwary R, Jeon S, Evans AC, Hess CP, Barkovich AJ, Xu D. NEOCIVET: towards accurate morphometry of neonatal gyrification and clinical applications in preterm newborns. *NeuroImage.* 2016;138:28–42.
- Kim H, Gano D, Ho ML, Guo XM, Unzueta A, Hess C, Ferriero DM, Xu D, Barkovich AJ. Hindbrain regional growth in preterm newborns and its impairment in relation to brain injury. *Hum Brain Mapp.* 2016;37:678–688.
- Kim SY, Liu M, Hong SJ, Toga AW, Barkovich AJ, Xu D, Kim H. Disruption and compensation of sulcation-based covariance networks in neonatal brain growth after perinatal injury. *Cereb Cortex.* 2020;30:6238–6253.
- Kinney HC, Brody BA, Kloman AS, Gilles FH. Sequence of central nervous system myelination in human infancy. II. Patterns of myelination in autopsied infants. *J Neuropathol Exp Neurol.* 1988;47:217–234.
- Kinney HC, Karthigasan J, Borenshteyn NI, Flax JD, Kirschner DA. Myelination in the developing human brain: biochemical correlates. *Neurochem Res.* 1994;19:983–996.
- Kirilina E, Helbling S, Morawski M, Pine K, Reimann K, Jankuhn S, Dinse J, Deistung A, Reichenbach JR, Trampel R, et al. Superficial white matter imaging: contrast mechanisms and whole-brain in vivo mapping. *Sci Adv.* 2020;6.
- Klein A, Andersson J, Ardekani BA, Ashburner J, Avants B, Chiang MC, Christensen GE, Collins DL, Gee J, Hellier P, et al. Evaluation of 14 nonlinear deformation algorithms applied to human brain MRI registration. *NeuroImage.* 2009;46:786–802.
- Kliegman RM, Hack M, Jones P, Fanaroff AA. Epidemiologic study of necrotizing enterocolitis among low-birth-weight infants. Absence of identifiable risk factors. *J Pediatr.* 1982;100:440–444.
- Laule C, Vavasour IM, Kolind SH, Li DK, Traboulsee TL, Moore GR, MacKay AL. Magnetic resonance imaging of myelin. *Neurotherapeutics.* 2007;4:460–484.
- Lebenberg J, Mangin J-F, Thirion B, Poupon C, Hertz-Pannier L, Leroy F, Adibpour P, Dehaene-Lambertz G, Dubois J. Mapping the asynchrony of cortical maturation in the infant brain: a MRI multi-parametric clustering approach. *NeuroImage.* 2019;185:641–653.
- Lee K, Cheral M, Budin F, Gilmore J, Coning KZ, Rasmussen J, Wadhwa PD, Entringer S, Glasser MF, Van Essen DC, et al. Early postnatal myelin content estimate of white matter via T1w/T2w ratio. *Proc SPIE Int Soc Optim Eng.* 2015:9417.
- Li G, Wang L, Shi F, Lyall AE, Ahn M, Peng Z, Zhu H, Lin W, Gilmore JH, Shen D. Cortical thickness and surface area in neonates at high risk for schizophrenia. *Brain Struct Funct.* 2016;221:447–461.
- Liu M, Lepage C, Jeon S, Flynn T, Yuan S, Kim J, Toga AW, Barkovich AJ, Xu D, Evans AC, editors. A skeleton and deformation based model for neonatal pial surface reconstruction

- in preterm newborns. In: 2019 IEEE 16th international symposium on biomedical imaging (ISBI 2019). IEEE; 2019. pp. 352–355. <https://doi.org/10.1109/ISBI.2019.8759183>.
- Liu M, Duffy BA, Sun Z, Toga AW, Barkovich AJ, Xu D, Kim H, editors. Deep learning of cortical surface features using graph-convolution predicts neonatal brain age and neurodevelopmental outcome. In: 2020 IEEE 17th international symposium on biomedical imaging (ISBI). IEEE, Iowa City, IA; 2020. pp. 1335–1338. <https://doi.org/10.1109/ISBI45749.2020.9098556>
- Liu M, Lepage C, Kim SY, Jeon S, Kim SH, Simon JP, Tanaka N, Yuan S, Islam T, Peng B. Robust cortical thickness morphometry of neonatal brain and systematic evaluation using multi-site MRI datasets. *Front Neurosci*. 2021;15:218.
- Lobel U, Sedlacik J, Gullmar D, Kaiser WA, Reichenbach JR, Mentzel HJ. Diffusion tensor imaging: the normal evolution of ADC, RA, FA, and eigenvalues studied in multiple anatomical regions of the brain. *Neuroradiology*. 2009;51:253–263.
- Ma Z, Zhang N. Cross-population myelination covariance of human cerebral cortex. *Hum Brain Mapp*. 2017;38:4730–4743.
- McKinstry RC, Mathur A, Miller JH, Ozcan A, Snyder AZ, Scheffert GL, Almlí CR, Shiran SI, Conturo TE, Neil JJ. Radial organization of developing preterm human cerebral cortex revealed by non-invasive water diffusion anisotropy MRI. *Cereb Cortex*. 2002;12:1237–1243.
- Mehlhorn AJ, Morin CE, Wong-You-Cheong JJ, Contag SA. Mild fetal cerebral ventriculomegaly: prevalence, characteristics, and utility of ancillary testing in cases presenting to a tertiary referral center. *Prenat Diagn*. 2017;37:647–657.
- Miller SP, Vigneron DB, Henry RG, Bohland MA, Ceppi-Cozzio C, Hoffman C, Newton N, Partridge JC, Ferriero DM, Barkovich AJ. Serial quantitative diffusion tensor MRI of the premature brain: development in newborns with and without injury. *J Magn Reson Imaging*. 2002;16:621–632.
- Mrzljak L, Uylings HB, Kostovic I, Van Eden CG. Prenatal development of neurons in the human prefrontal cortex: I. a qualitative golgi study. *J Comp Neurol*. 1988;271:355–386.
- Nakamura K, Chen JT, Ontaneda D, Fox RJ, Trapp BD. T1–/T2-weighted ratio differs in demyelinated cortex in multiple sclerosis. *Ann Neurol*. 2017;82:635–639.
- Norbom LB, Rokicki J, Alnaes D, Kaufmann T, Doan NT, Andreassen OA, Westlye LT, Tamnes CK. Maturation of cortical microstructure and cognitive development in childhood and adolescence: a T1w/T2w ratio MRI study. *Hum Brain Mapp*. 2020;41:4676–4690.
- Nossin-Manor R, Card D, Morris D, Noormohamed S, Shroff MM, Whyte HE, Taylor MJ, Sled JG. Quantitative MRI in the very preterm brain: assessing tissue organization and myelination using magnetization transfer, diffusion tensor and T(1) imaging. *NeuroImage*. 2013;64:505–516.
- Oishi K, Mori S, Donohue PK, Ernst T, Anderson L, Buchthal S, Faria A, Jiang H, Li X, Miller MI, et al. Multi-contrast human neonatal brain atlas: application to normal neonate development analysis. *NeuroImage*. 2011;56:8–20.
- Ortinau C, Neil J. The neuroanatomy of prematurity: normal brain development and the impact of preterm birth. *Clin Anat*. 2015;28:168–183.
- Ouyang M, Dubois J, Yu Q, Mukherjee P, Huang H. Delineation of early brain development from fetuses to infants with diffusion MRI and beyond. *NeuroImage*. 2019;185:836–850.
- Ouyang M, Jeon T, Sotiras A, Peng Q, Mishra V, Halovanic C, Chen M, Chalak L, Rollins N, Roberts TPL, et al. Differential cortical microstructural maturation in the preterm human brain with diffusion kurtosis and tensor imaging. *Proc Natl Acad Sci U S A*. 2019;116:4681–4688.
- Oyefiade AA, Ameis S, Lerch JP, Rockel C, Szulc KU, Scantlebury N, Decker A, Jefferson J, Spichak S, Mabbott DJ. Development of short-range white matter in healthy children and adolescents. *Hum Brain Mapp*. 2018;39:204–217.
- Pacheco J, Goh JO, Kraut MA, Ferrucci L, Resnick SM. Greater cortical thinning in normal older adults predicts later cognitive impairment. *Neurobiol Aging*. 2015;36:903–908.
- Partridge SC, Mukherjee P, Henry RG, Miller SP, Berman JI, Jin H, Lu Y, Glenn OA, Ferriero DM, Barkovich AJ, et al. Diffusion tensor imaging: serial quantitation of white matter tract maturity in premature newborns. *NeuroImage*. 2004;22:1302–1314.
- Pecheva D, Kelly C, Kimpton J, Bonthron A, Batalle D, Zhang H, Counsell SJ. Recent advances in diffusion neuroimaging: applications in the developing preterm brain. *F1000Research*. 2018;7.
- Petracca M, El Mendili MM, Moro M, Cocozza S, Podranski K, Fleysher L, Inglese M. Laminar analysis of the cortical T1/T2-weighted ratio at 7T. *Neurol Neuroimmunol Neuroinflamm*. 2020;7.
- Phillips OR, Clark KA, Luders E, Azhir R, Joshi SH, Woods RP, Mazziotta JC, Toga AW, Narr KL. Superficial white matter: effects of age, sex, and hemisphere. *Brain Connect*. 2013;3:146–159.
- Rakic P. Developmental and evolutionary adaptations of cortical radial glia. *Cereb Cortex*. 2003;13:541–549.
- Righart R, Biberacher V, Jonkman LE, Klaver R, Schmidt P, Buck D, Berthele A, Kirschke JS, Zimmer C, Hemmer B, et al. Cortical pathology in multiple sclerosis detected by the T1/T2-weighted ratio from routine magnetic resonance imaging. *Ann Neurol*. 2017;82:519–529.
- Schmithorst VJ, Yuan W. White matter development during adolescence as shown by diffusion MRI. *Brain Cogn*. 2010;72:16–25.
- Schneider J, Kober T, Bickle Graz M, Meuli R, Huppi PS, Hagmann P, Truttmann AC. Evolution of T1 relaxation, ADC, and fractional anisotropy during early brain maturation: a serial imaging study on preterm infants. *AJNR Am J Neuroradiol*. 2016;37:155–162.
- Shafee R, Buckner RL, Fischl B. Gray matter myelination of 1555 human brains using partial volume corrected MRI images. *NeuroImage*. 2015;105:473–485.
- Sierra M, Nestler S, Jay EL, Ecker C, Feng Y, David AS. A structural MRI study of cortical thickness in depersonalisation disorder. *Psychiatry Res*. 2014;224:1–7.
- Smith SM. Fast robust automated brain extraction. *Hum Brain Mapp*. 2002;17:143–155.
- Smith SM, Jenkinson M, Woolrich MW, Beckmann CF, Behrens TE, Johansen-Berg H, Bannister PR, De Luca M, Drobnjak I, Flitney DE, et al. Advances in functional and structural MR image analysis and implementation as FSL. *NeuroImage*. 2004;23(Suppl 1):S208–S219.
- Smyser TA, Smyser CD, Rogers CE, Gillespie SK, Inder TE, Neil JJ. Cortical gray and adjacent white matter demonstrate synchronous maturation in very preterm infants. *Cereb Cortex*. 2016;26:3370–3378.
- Song S-K, Sun S-W, Ju W-K, Lin S-J, Cross AH, Neufeld AH. Diffusion tensor imaging detects and differentiates axon and myelin degeneration in mouse optic nerve after retinal ischemia. *NeuroImage*. 2003;20:1714–1722.
- Song S-K, Yoshino J, Le TQ, Lin S-J, Sun S-W, Cross AH, Armstrong RC. Demyelination increases radial diffusivity in corpus callosum of mouse brain. *NeuroImage*. 2005;26:132–140.
- Soun JE, Liu MZ, Cauley KA, Grinband J. Evaluation of neonatal brain myelination using the T1- and T2-weighted MRI ratio. *J Magn Reson Imaging*. 2017;46:690–696.
- Teubner-Rhodes S, Vaden KI Jr, Cute SL, Yeatman JD, Dougherty RF, Eckert MA. Aging-resilient associations between the arcuate

- fasciculus and vocabulary knowledge: microstructure or morphology? *J Neurosci*. 2016;36:7210–7222.
- Timmler S, Simons M. Grey matter myelination. *Glia*. 2019;67:2063–2070.
- Tzourio-Mazoyer N, Landeau B, Papathanassiou D, Crivello F, Etard O, Delcroix N, Mazoyer B, Joliot M. Automated anatomical labeling of activations in SPM using a macroscopic anatomical parcellation of the MNI MRI single-subject brain. *NeuroImage*. 2002;15:273–289.
- Uddin MN, Figley TD, Solar KG, Shatil AS, Figley CR. Comparisons between multi-component myelin water fraction, T1w/T2w ratio, and diffusion tensor imaging measures in healthy human brain structures. *Sci Rep*. 2019;9:2500.
- van den Heuvel MP, Kersbergen KJ, de Reus MA, Keunen K, Kahn RS, Groenendaal F, de Vries LS, Benders MJ. The neonatal connectome during preterm brain development. *Cereb Cortex*. 2015;25:3000–3013.
- Van Essen DC, Smith SM, Barch DM, Behrens TE, Yacoub E, Ugurbil K, Consortium WU-MH. The WU-Minn human connectome project: an overview. *NeuroImage*. 2013;80:62–79.
- Volpe JJ. Neurology of the newborn. *Major Probl Clin Pediatr*. 1981;22:1–648.
- Volpe JJ. Brain injury in the premature infant—from pathogenesis to prevention. *Brain Dev*. 1997;19:519–534.
- Volpe JJ. Brain injury in premature infants: a complex amalgam of destructive and developmental disturbances. *Lancet Neurol*. 2009;8:110–124.
- Volpe JJ, Kinney HC, Jensen FE, Rosenberg PA. Reprint of “The developing oligodendrocyte: key cellular target in brain injury in the premature infant”. *Int J Dev Neurosci*. 2011;29:565–582.
- Wang H, Yushkevich PA. Multi-atlas segmentation with joint label fusion and corrective learning—an open source implementation. *Front Neuroinform*. 2013;7:27.
- Wilson S, Pietsch M, Cordero-Grande L, Price AN, Hutter J, Xiao J, McCabe L, Rutherford MA, Hughes EJ, Counsell SJ. Development of human white matter pathways in utero over the second and third trimester. *PNAS*. 2021:118.
- Wimberger DM, Roberts TP, Barkovich AJ, Prayer LM, Moseley ME, Kucharczyk J. Identification of “premyelination” by diffusion-weighted MRI. *J Comput Assist Tomogr*. 1995;19:28–33.
- Wright R, Kyriakopoulou V, Ledig C, Rutherford MA, Hajnal JV, Rueckert D, Aljabar P. Automatic quantification of normal cortical folding patterns from fetal brain MRI. *NeuroImage*. 2014;91:21–32.
- Wu M, Lu LH, Lowes A, Yang S, Passarotti AM, Zhou XJ, Pavuluri MN. Development of superficial white matter and its structural interplay with cortical gray matter in children and adolescents. *Hum Brain Mapp*. 2014;35:2806–2816.
- Yu Q, Ouyang A, Chalak L, Jeon T, Chia J, Mishra V, Sivaranjan M, Jackson G, Rollins N, Liu S, et al. Structural development of human fetal and preterm brain cortical plate based on population-averaged templates. *Cereb Cortex*. 2016;26:4381–4391.